Article

Discovery Medicine 2024; 36(191): 2408–2420
https://doi.org/10.24976/Discov.Med.202436191.222

KDM4C and *GFPT1*: Potential Therapeutic Targets for Gastric Cancer

Chenkai Li[1,†], Yunqian Chu[2,†], Hanjue Dai[2], Qingying Xian[2], Wenyu Zhu[2,*]

[1]Department of Science and Technology, The Affiliated Changzhou No.2 People's Hospital of Nanjing Medical University, 213003 Changzhou, Jiangsu, China
[2]Department of Oncology, The Affiliated Changzhou No.2 People's Hospital of Nanjing Medical University, 213003 Changzhou, Jiangsu, China
*Correspondence: zhuwenyu_zwyy@163.com (Wenyu Zhu)
[†]These authors contributed equally.
Published: 20 December 2024

Background: Detecting and treating stomach cancer requires a comprehensive understanding of how gastric cancer develops and progresses. In this context, efforts have been made to elucidate the regulation of glutamine-fructose-6-phosphate transaminase 1 (*GFPT1*) and Lysine demethylase 4C (*KDM4C*) in gastric cancer.
Methods: Bioinformatics was utilized to predict the levels and correlation of *GFPT1* and *KDM4C* in gastric cancer, followed by determining their expressions via quantitative real-time polymerase chain reaction (qRT-PCR). The viability (assessed through Cell Counting Kit-8 (CCK-8) assay), proliferation (via colony-forming assay), migration, and invasion (utilizing transwell assay), as well as vasculogenic mimicry (examined through Tube formation assay), in gastric cancer cells, were quantified. Additionally, quantification of *GFPT1* and proliferation/epithelial-mesenchymal transition (EMT)-related proteins was conducted through Western blot analysis.
Results: In gastric cancer cells, *GFPT1* was found to be abundantly expressed. Overexpression of *GFPT1* resulted in increased viability, proliferation, migration, invasion, vasculogenic mimicry, and EMT of gastric cancer cells, while knockdown of *GFPT1* had the opposite effects. Moreover, there was a positive correlation between *KDM4C* and *GFPT1* in gastric cancer. Overexpression of *KDM4C* led to increased expression of *GFPT1* and enhanced the aforementioned effects of *GFPT1* overexpression, whereas knockdown of *KDM4C* produced inverse effects. Interestingly, the effects of *KDM4C* overexpression combined with *GFPT1* knockdown, or *GFPT1* overexpression combined with *KDM4C* knockdown, could mutually reverse their effects on the aforementioned cell phenotypes.
Conclusion: *KDM4C* positively regulates *GFPT1*, thereby promoting gastric cancer progression. This discovery provides a new avenue for slowing down the progression of gastric cancer.

Keywords: gastric cancer; glutamine-fructose-6-phosphate transaminase 1; Lysine demethylase 4C; vasculogenic mimicry; epithelial-mesenchymal transition

Introduction

Gastric cancer ranks as the third most common cause of cancer-related deaths and poses a significant threat to the digestive system. According to a 2018 statistical report, gastric cancer accounted for 8.2% of global cancer cases, resulting in over 783,000 fatalities [1]. The study has indicated that gastric cancer often develops from precursor lesions, including *H. pylori*-related chronic atrophic gastritis and autoimmune chronic atrophic gastritis [2]. Recent research has shown that only 25% of gastric cancer cases worldwide survive for five years or more. Despite the availability of multiple treatment options, the survival rate remains unsatisfactory [3].

Intestinal or incomplete metaplasia of the gastric mucosa is known to be a precursor to gastric cancer [4]. Cancer cells often undergo significant transformations through a cellular process known as epithelial-mesenchymal transition (EMT) [5]. EMT is characterized as a reversible process wherein epithelial cells adopt a spindle-shaped, mesenchymal morphology. The malignant progression of many cancers is likely dependent on the activation of EMT [6]. Glutamine-fructose-6-phosphate transaminase 1 (*GFPT1*) serves as the initiation and rate-limiting enzyme of the hexosamine biosynthetic pathway (HBP). HBP is involved in the metabolic processes of cancer cells, utilizing glucose. *GFPT1* catalyzes the conversion of glutamine and fructose-6-phosphate into glucosamine-6-phosphate, a key regulator for the entry of glucose into the HBP pathway [7]. It has been established that several disorders, including esophageal cancer, hepatocellular carcinoma, and prostate cancer, are associated with *GFPT1* expression [8–10]. Furthermore, database prediction results have indicated abun-

dant expression of *GFPT1* in gastric cancer. Accordingly, we have elucidated how *GFPT1* contributes to the growth of gastric cancer.

Epigenetics lies at the heart of gastric cancer research. In recent years, novel treatments targeting histone methylation have emerged [11]. Typically, histone methylation occurs in the promoter region of active genes, thereby labeling active transcription sites. Histone methylation generally exerts a stable directional influence on gene transcription and can have highly variable effects on gene expression [12]. Specifically, histone H3 is methylated on lysine 36 (H3K36) within open chromatin, which serves to activate transcription, inhibit enzyme activity, and prevent aberrant transcription by recruiting regulatory proteins that influence chromatin structure [12,13].

The epigenetic role of histone H3 trimethylated at lysine 36 (H3K36me3) is crucial for maintaining genomic stability, with defects associated with various human diseases, including prenatal developmental disorders [14] and cancer [15–17]. Through analysis using the Cistrome DB, the enrichment of histone methylation modifications in several *GFPT1* promoter regions has been compared, revealing that H3K36me3 exhibits the highest enrichment. Additionally, hTFtarget analysis (https://guolab.wchscu.cn/hTFtarget/#!/) has indicated that the H3K36me3-associated transferase, Lysine demethylase 4C (*KDM4C*), is enriched in the *GFPT1* promoter region. The Jumonji domain-2 family of histone demethylases includes *KDM4C*, once considered an oncogene, with its deregulation linked to numerous malignancies and tumors [18]. Notably, *KDM4C* has been found to accelerate the development of gastric cancer [19].

As a consequence, we hypothesized that *KDM4C* may regulate *GFPT1* and influence the viability, migration, proliferation, invasion, and vascular mimicry of gastric cancer cells.

Materials and Methods

Bioinformatics Analysis

Analysis conducted using the starBase database (http://starbase.sysu.edu.cn) revealed the expression of *GFPT1* or *KDM4C* in gastric cancer tissues. The GEPIA database (http://gepia.cancer-pku.cn/) was used to detect the correlation between *GFPT1* and *KDM4C* expression in gastric cancer.

Plasmid Construction

The *GFPT1* overexpression plasmid (RC207225), small interfering RNA targeting *GFPT1* (si-*GFPT1*) (SR301783), *KDM4C* overexpression plasmid (RC211182), and si-*KDM4C* (SR307990) were procured from OriGene (Rockville, MD, USA). The sequences of the siRNAs were designed using the siRNA Target Finder (https://www.genscript.com/). The sequences for *GFPT1* and *KDM4C* siRNAs were 5′-AAGTCAAGATACCAGCTTTAC-3′ and 5′-AACATAGCTCGCCTCAATACA-3′, respectively. The pCMV6-Entry vector (PS100001, OriGene, Rockville, MD, USA) served as a negative control (NC) for *GFPT1* and *KDM4C* overexpression experiments. The si-NC (SR30004, OriGene, Rockville, MD, USA) was used as the control of si-*GFPT1* and si-*KDM4C*.

Cell Culture and Transfection

Culture of GES-1 (IM-H084, Immocell, Xiamen, China), AGS (CRL-1739, American Type Culture Collection (ATCC), Rockefeller, MD, USA), SNU-5 (CRL-5973, ATCC, Rockefeller, MD, USA), NCI-N87 (CRL-5822, ATCC, Rockefeller, MD, USA), and MKN45 (C6591, Beyotime, Shanghai, China), was conducted in RPMI 1640 complete medium (11875119, ThermoFisher, Waltham, MA, USA) supplemented with 10% fetal bovine serum (FBS) (12103C, Merck KGaA, Darmstadt, Germany) under standard conditions (37 °C, 5% CO_2). All cell lines utilized in this study were confirmed to be mycoplasma-free and authenticated via short tandem repeat (STR) profiling.

Cell transfection was carried out in two stages. In the first stage, transfection with si-*GFPT1*/si-NC and *GFPT1*/NC was conducted in AGS and MKN45 cells, respectively. In the second stage, transfection of si-NC+NC/si-*GFPT1*+NC/si-NC+*KDM4C*/si-*GFPT1*+*KDM4C* was performed in AGS cells, while si-NC+NC/NC+si-*KDM4C*/*GFPT1*+si-NC/*GFPT1*+si-*KDM4C* transfection was performed on MKN45 cells.

Quantitative Real-Time Polymerase Chain Reaction (qRT-PCR)

Total RNA isolation from GES-1, AGS, SNU-5, NCI-N87, and MKN45 cells was performed using the TRIzol reagent (AM9738, ThermoFisher, Waltham, MA, USA), followed by cDNA synthesis using a specific kit (K1622, ThermoFisher, Waltham, MA, USA). Subsequently, qRT-PCR amplification with cDNA was carried out using Fast SYBR green master mix (4385610, ThermoFisher, Waltham, MA, USA) under the following conditions: predenaturation at 94 °C for 2 min, followed by 40 cycles of denaturation at 94 °C for 15 sec, annealing at 60 °C for 1 min, and elongation at 72 °C for 1 min. Data acquisition was performed using a qRT-PCR apparatus (CFX Opus Deepwell Real-Time PCR System, Bio-Rad Laboratories, Hercules, CA, USA), and analysis was conducted using the $2^{-\triangle\triangle CT}$ method [20]. Table 1 provides a list of the primers used in the study.

Cell Counting Kit-8 (CCK-8) Assay

AGS and MKN45 cells, following the aforementioned transfection, were plated in 96-well plates at a density of 5 $\times$ 10^3 cells per well and incubated at 37 °C with 5% CO_2. Detection was performed at 24- and 48-h post-transfection. Cells were then incubated at 37 °C for 1 hour in wells

Table 1. Primers used in quantitative real-time polymerase chain reaction.

Primer name		Sequence (5′–3′)
GFPT1	F	GGAAGCCAATGCCTGCAAAA
	R	GTGATCCCCACCGTGTGAAT
KDM4C	F	AACCTCTAAGAGTTGGCGCC
	R	TCTGCTGTCCACGCATTTCT
GADPH	F	CATGGGTGTGAACCATGAGA
	R	CAGTGATGGCATGACTGTG

Abbreviations: *GFPT1*, glutamine-fructose-6-phosphatase aminotransferase 1; *KDM4C*, Lysine demethylase 4C; *GADPH*, glyceraldehyde-3-phosphate dehydrogenase; F, forward; R, reverse.

containing 10 µL of CCK-8 solution (C0038, Beyotime, China). Absorbance measurements at 450 nm were conducted using a microplate reader (HTS-XT, BrukerOptics, Rheinstetten, Germany).

Colony-Forming Assay

After reaching the logarithmic growth phase and digestion with 0.25% trypsin (15050065, ThermoFisher, Waltham, MA, USA), transfected AGS and MKN45 cells were suspended in RPMI-1640 supplemented with 10% FBS. The cells were then seeded in 6-well plates (700 cells per well) and incubated for 2–3 weeks at 37 °C with 5% CO_2 and saturated humidity, with medium refreshed every three days. Subsequently, cell tests were performed. After cloning and washing with phosphate-buffered saline (PBS) (P4474, Merck KGaA, Darmstadt, Germany), cells were fixed in 1 mL of 4% paraformaldehyde (P6148, Merck KGaA, Darmstadt, Germany) for 30–60 min and then subjected to color development for 10–20 min in 1 mL of 1% crystal violet staining solution (HT90132, Merck KGaA, Darmstadt, Germany). After repeated PBS washes, the cells were air-dried. Pictures of the cells were captured using a microscope (Mateo TL, Leica Microsystems, Solms, Germany).

Transwell Migration

Transfected AGS and MKN45 cells were cultured until reaching the logarithmic growth phase. Subsequently, the cells were washed with 1% PBS and treated with 0.25% trypsin (15050065, ThermoFisher, Waltham, MA, USA) for digestion. To neutralize the trypsin, 0.5 mg/mL trypsin inhibitor (R007100, ThermoFisher, Waltham, MA, USA) was added to PBS. The cells were gently pipetted to disperse them into individual cells as much as possible. Afterward, the cells were washed twice with DMEM (12491015, ThermoFisher, Waltham, MA, USA) containing 0.5% FBS (12103C, Merck KGaA, Darmstadt, Germany) to remove residual trypsin and inhibitors.

In 24-well transwell chambers (8 µm-pore, 3422, CORNING, New York, NY, USA), the lower compartment was filled with 500 µL of DMEM supplemented with 10% FBS, while the upper chamber contained 100 µL of culture medium containing 1×10^5 cells. The chambers were then incubated at 37 °C with 5% CO_2. After 48 hours, non-invading cells on the membrane were carefully removed. Cells in the lower chamber were fixed with 4% paraformaldehyde for 1 hour and then stained with 1% crystal violet in 2% ethanol (51976, Merck KGaA, Darmstadt, Germany) for 20 min. Excess water was drained from one side of the chamber using a cotton swab. The cells were then photographed under a microscope at 250× magnification (Mateo TL, Leica Microsystems, Germany), and quantification was performed using Image J software (version 2.0, National Institutes of Health, Bethesda, MD, USA).

Transwell Invasion

Transfected AGS and MKN45 cells in the logarithmic growth phase were prepared for invasion assays. Matrigel-coated Transwell chambers (3422, CORNING, USA) were utilized for these tests. The lower compartment was filled with 500 µL of DMEM containing 10% FBS, while the upper compartment contained 100 µL of serum-free media and 1×10^5 cells. The chambers were then transferred to a 5% CO_2 incubator and cultured for 48 hours at 37 °C. Only cells that passed through the membrane were fixed with 4% paraformaldehyde (P6148, Merck KGaA, Darmstadt, Germany) and stained with 1% crystal violet (HT90132, Merck KGaA, Darmstadt, Germany). Subsequently, the cells were photographed under a microscope at 250× magnification (Mateo TL, Leica Microsystems, Germany) and quantified using Image J software (National Institutes of Health, Bethesda, USA).

Tube Formation Assay

AGS and MKN45 cells were transfected as described above. Human umbilical vein endothelial cells (HUVECs, CBP60340, COBIOER, Nanjing, China) were cultured in BEGM™ Bronchial Epithelial Cell Growth Medium BulletKit™ (CC-3170, Lonza, Basel, Switzerland) and passaged from the 2nd to the 6th generation for experimentation. On the day prior to the experiment, serum-deprived cells and matrigel (356231, CORNING, USA) were placed in an icebox at 4 °C overnight to allow the matrigel to slowly melt. Both gastric cancer cell lines and HUVECs were cultured in a normoxic incubator. After 24 hours, the supernatant of gastric cancer cells was centrifuged to remove cells. HUVECs were then digested and resuspended with the supernatant to a density of 1×10^4 cells/mL. Subsequently, 50 µL of matrigel was added to each well and placed in a cell incubator for 60 min to solidify. Following solidification, 100 µL of the cell suspension (1×10^4 cells/well) was added to each well, and the cells were incubated for 12 hours. Tube structures were then captured using a microscope (×100 magnification, Mateo TL, Le-

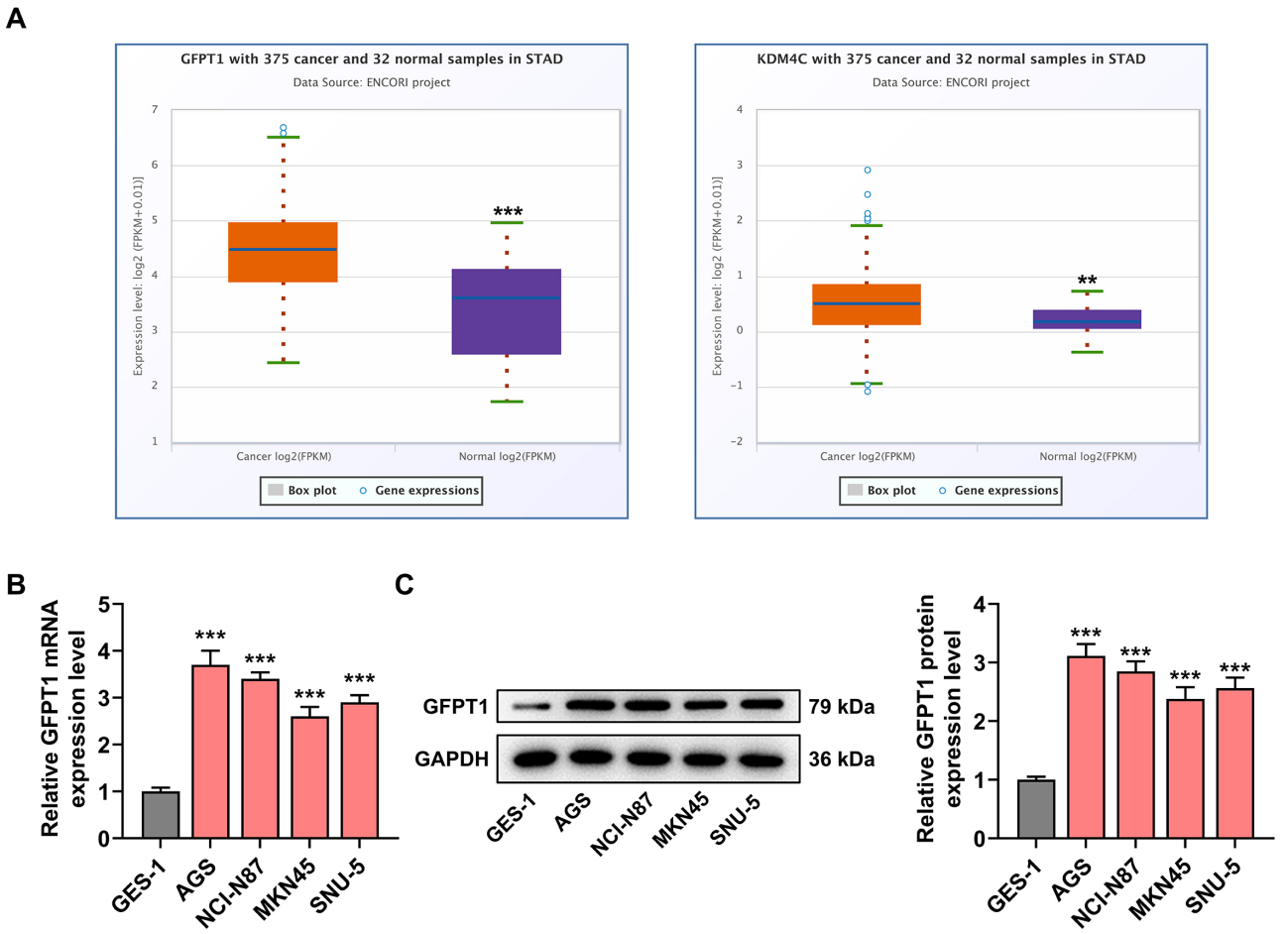

Fig. 1. *GFPT1* was highly expressed in gastric cancer cells. (A) Prediction on *GFPT1* (left) or *KDM4C* (right) expression in gastric cancer tissues (starBase database). (B,C) *GFPT1* expression in gastric cancer cell lines and normal gastric mucosal cell lines (quantitative real-time polymerase chain reaction and Western blot). ***$p < 0.001$, **$p < 0.01$; * vs GES-1 or Cancer. n = 3. Abbreviation: *GFPT1*, glutamine-fructose-6-phosphate transaminase 1; NC, negative control.

ica Microsystems, Germany), and quantification was performed using the National Institutes of Health's Image J software.

Western Blot Analysis

GES-1, AGS, SNU-5, NCI-N87, and MKN45 cells, transfected with GFPT1, AGS cells transfected with si-*GFPT1*, si-NC, si-NC+NC, si-NC+*KDM4C*, si-*GFPT1*+NC, and si-*GFPT1*+*KDM4C*, and MKN45 cells transfected with NC, *GFPT1*, si-NC+NC, NC+si-*KDM4C*, *GFPT1*+si-NC, and *GFPT1*+si-*KDM4C* underwent protein extraction using Radioimmunoprecipitation Assay (RIPA) Lysis Buffer (R0010, Solarbio, Beijing, China). The protein concentration was determined using the Bicinchoninic Acid (BCA) Protein Assay Kit (23227, ThermoFisher, Waltham, MA, USA).

Protein samples were separated by SDS-PAGE (EA0355BOX, ThermoFisher, Waltham, MA, USA) and terminated by electrophoresis once the bromophenol blue dye reached the end of the gel. The proteins were then transferred to polyvinylidene fluoride membranes (BSP0161, Solarbio, Beijing, China) after rinsing off the unstained dye with water. Following a 1-h blocking step with 5% bovine serum albumin (BSA) (A1933, Merck KGaA, Darmstadt, Germany), the membranes were incubated first with primary antibodies overnight at 4 °C, followed by incubation with secondary antibodies at room temperature for 60 min. The membrane was then visualized using an enhanced chemiluminescent (ECL) kit (WP20005, ThermoFisher, Waltham, MA, USA). Images were acquired using a gel imager (A44116, ThermoFisher, Waltham, MA, USA), and the gray values were analyzed using the Image J analysis program (National Institutes of Health, Bethesda, USA).

The relative value of the target protein was calculated and normalized using the following formula: relative gray value = gray value of target band / gray value of internal control (GAPDH).

Except for EphA2 (6997T, 1:1000, 125 kDa, CST, Danvers, MA, USA), all antibodies used were ordered

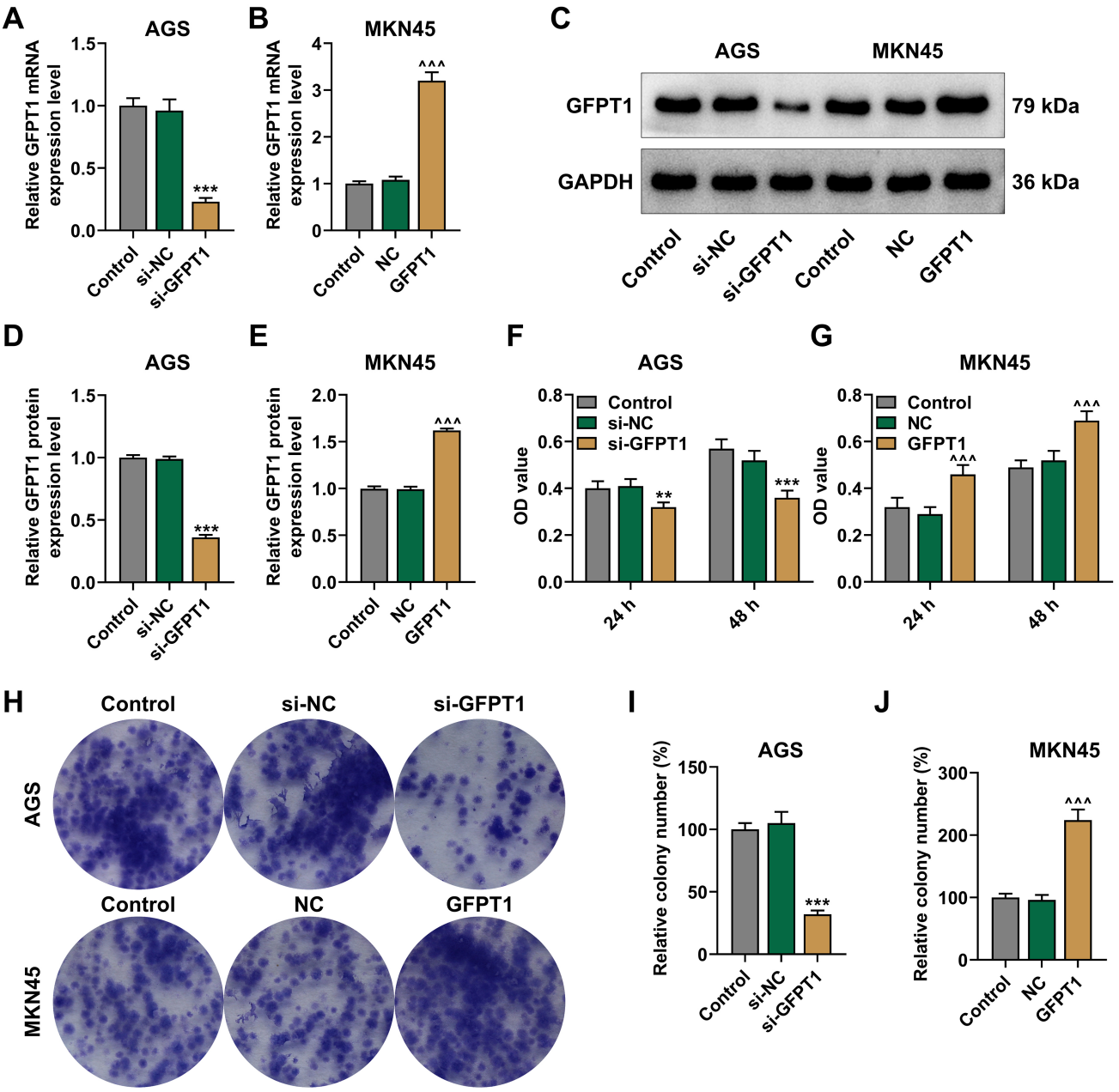

Fig. 2. Effects of *GFPT1* on gastric cancer cell viability and proliferation. AGS and MKN45 cells received transfection of si-*GFPT1* and *GFPT1* overexpression plasmid, respectively. (A–E) *GFPT1* expression in AGS and MKN45 cells (quantitative real-time polymerase chain reaction and Western blot). (F,G) Effects of *GFPT1* on AGS and MKN45 cell viability (Cell Counting Kit-8 assay). (H–J) Effects of *GFPT1* on AGS and MKN45 cell proliferation (colony-forming assay). $^{\wedge\wedge\wedge}p < 0.001$, $***p < 0.001$, $**p < 0.01$; * vs si-NC, $^{\wedge}$ vs NC. n = 3. Abbreviation: *GFPT1*, glutamine-fructose-6-phosphate transaminase 1; NC, negative control.

from Abcam (Cambridge, UK). These include GFPT1 (ab125069, 1:200, 79 kDa), Ki67 (ab92742, 1:5000, 359 kDa), E-cadherin (ab40772, 1:1000, 97 kDa), N-cadherin (ab98952, 1:500, 100 kDa), Vimentin (ab137321, 1:500, 54 kDa), VE-cadherin (ab33168, 1 µg/mL, 115 kDa), GAPDH (ab8245, 1:500, 36 kDa), goat anti-rabbit IgG H&L (ab6721, 1:2000, 37 kDa), and goat anti-mouse IgG H&L (ab205719, 1:2000, 52 kDa).

Statistical Analysis

Statistical analyses were completed using SPSS 20.0 (IBM SPSS Inc., Chicago, IL, USA). Measurement data were presented as mean ± standard deviation. Comparative data from multiple groups were analyzed using a one-way analysis of variance. Significance was defined as $p < 0.05$.

Results

GFPT1 was Abundantly Expressed in Gastric Cancer Cell Lines

Predictions from the starBase database indicated significantly higher *GFPT1* (left) or *KDM4C* (right) expression in gastric cancer tissues compared to healthy tissues ($p < 0.01$, Fig. 1A). Subsequent analysis of *GFPT1* expression using qRT-PCR and Western blot revealed elevated levels in gastric cancer cell lines AGS, NCI-N87, MKN45, and SNU-5, relative to normal gastric mucosal cell line GES-1 ($p < 0.001$, Fig. 1B,C).

GFPT1 can Boost Malignant Behaviors of Gastric Cancer Cells, and Increase Proliferation/EMT-Related Protein Expressions

The transfection efficiency of *GFPT1* and si-*GFPT1* into gastric cancer cells AGS and MKN45 was assessed using qRT-PCR and Western blot analyses. si-*GFPT1* significantly reduced the level of *GFPT1* expression ($p < 0.001$, Fig. 2A–E), while *GFPT1* overexpression had the opposite effect ($p < 0.001$, Fig. 2A–E). According to the CCK-8 assay, *GFPT1* silencing led to decreased AGS cell viability at 24 and 48 hours ($p < 0.01$, Fig. 2F), whereas *GFPT1* overexpression notably enhanced MKN45 cell viability ($p < 0.001$, Fig. 2G). Data from the colony-forming experiment demonstrated suppressed proliferation of AGS cells following *GFPT1* silencing ($p < 0.001$, Fig. 2H,I), while overexpression of *GFPT1* promoted proliferation of MKN45 cells ($p < 0.001$, Fig. 2H,J).

Using the transwell assay, gastric cancer cell migration and invasion were evaluated. Silencing of *GFPT1* decreased AGS cell migration, whereas overexpression of *GFPT1* increased MKN45 cell migration ($p < 0.001$, Fig. 3A–C). Additionally, *GFPT1* silencing reduced AGS cell invasion ($p < 0.001$, Fig. 3D,E), while *GFPT1* overexpression enhanced MKN45 cell invasion ($p < 0.001$, Fig. 3D,F), as observed in the transwell assay data.

Results from the tube formation assay confirmed that silencing of *GFPT1* suppressed the vasculogenic mimicry of AGS cells ($p < 0.001$, Fig. 3G,H), whereas its overexpression promoted the vasculogenic mimicry of MKN45 cells ($p < 0.001$, Fig. 3G,I).

Quantification of Ki67, E-cadherin, N-cadherin, Vimentin, VE-cadherin, and EphA2 was conducted via Western blot analysis. In AGS cells, *GFPT1* knockdown resulted in reduced expressions of Ki67, N-cadherin, Vimentin, VE-cadherin, and EphA2, while increasing the level of E-cadherin ($p < 0.001$, Fig. 4A,B). Conversely, in MKN45 cells, overexpression of *GFPT1* led to elevated levels of Ki67, N-cadherin, Vimentin, VE-cadherin, and EphA2, accompanied by decreased expression of E-cadherin ($p < 0.001$, Fig. 4A,C). These findings indicate that *GFPT1* plays a role in promoting EMT in gastric cancer cells.

KDM4C can Boost the Development of Gastric Cancer by Upregulation of GFPT1

The GEPIA database revealed a significant interaction between *KDM4C* and *GFPT1* in gastric cancer ($p = 2.6 \times 10^{-11}$, Fig. 4D). In AGS cells, compared to the si-NC+NC or si-*GFPT1*+NC group, overexpression of *KDM4C* significantly upregulated *KDM4C* levels in the si-NC+*KDM4C* or si-*GFPT1*+*KDM4C* group ($p < 0.001$, Fig. 5A). Similarly, in MKN45 cells, silencing of *KDM4C* markedly reduced *KDM4C* levels in the NC+si-*KDM4C* and *GFPT1*+si-*KDM4C* groups compared to the NC+si-NC and *GFPT1*+si-NC groups ($p < 0.001$, Fig. 5B). However, *GFPT1* expression had no effect on *KDM4C* levels (Fig. 5A,B). Furthermore, in contrast to the si-NC+NC or si-*GFPT1*+NC group, overexpression of *KDM4C* increased *GFPT1* levels in AGS cells of the si-NC+*KDM4C* and si-*GFPT1*+*KDM4C* groups ($p < 0.001$, Fig. 5C). *KDM4C* silencing significantly decreased *GFPT1* expression in MKN45 cells; however, overexpression of *GFPT1* reversed the effect of *KDM4C* silencing ($p < 0.001$, Fig. 5D).

The vitality and proliferation of AGS cells were stronger in the si-NC+*KDM4C* group, but were weaker in the si-*GFPT1*+NC group; moreover, *GFPT1* silencing reversed the roles of *KDM4C* overexpression in AGS cell vitality ($p < 0.001$, Fig. 5E) and proliferation ($p < 0.001$, Fig. 5G,H). MKN45 cell viability was weakened by transfection with NC+si-*KDM4C* while being enhanced by transfection with *GFPT1*+si-NC ($p < 0.05$, Fig. 5F). Also, overexpressed *GFPT1* offset the role of *KDM4C* silencing in MKN45 cell viability ($p < 0.001$, Fig. 5F) and proliferation ($p < 0.01$, Fig. 5G,I).

Cell migration and invasion were assessed using the transwell assay. AGS cells transfected with si-NC+*KDM4C* exhibited robust migratory and invasive capacities, whereas weaker capacities were observed in AGS cells transfected with si-*GFPT1*+NC. Additionally, *KDM4C* overexpression attenuated the effect of *GFPT1* knockdown on cell migration and invasion ($p < 0.001$, Fig. 6A,B,D,E). In contrast, MKN45 cells transfected with NC+si-*KDM4C* showed reduced migration and invasion abilities, but these abilities were potentiated by transfection with *GFPT1*+si-NC ($p < 0.001$, Fig. 6A,C,D,F). Moreover, MKN45 cells in the *GFPT1*+si-*KDM4C* group exhibited enhanced migration and invasion compared to the NC+si-*KDM4C* group, yet inhibited relative to the *GFPT1*+si-NC group ($p < 0.01$, Fig. 6A,C,D,F).

The vasculogenic mimicry of AGS and MKN45 cells was assessed using the tube formation assay. The length of blood vessels generated by co-culturing HUVEC with AGS cells transfected with si-NC+*KDM4C* was significantly increased, whereas it was diminished by transfection with si-*GFPT1*+NC ($p < 0.01$, Fig. 6G,H). AGS cells transfected with si-*GFPT1*+*KDM4C* exhibited blood vessels that were substantially shorter than those transfected with si-NC+*KDM4C* and longer than those transfected with

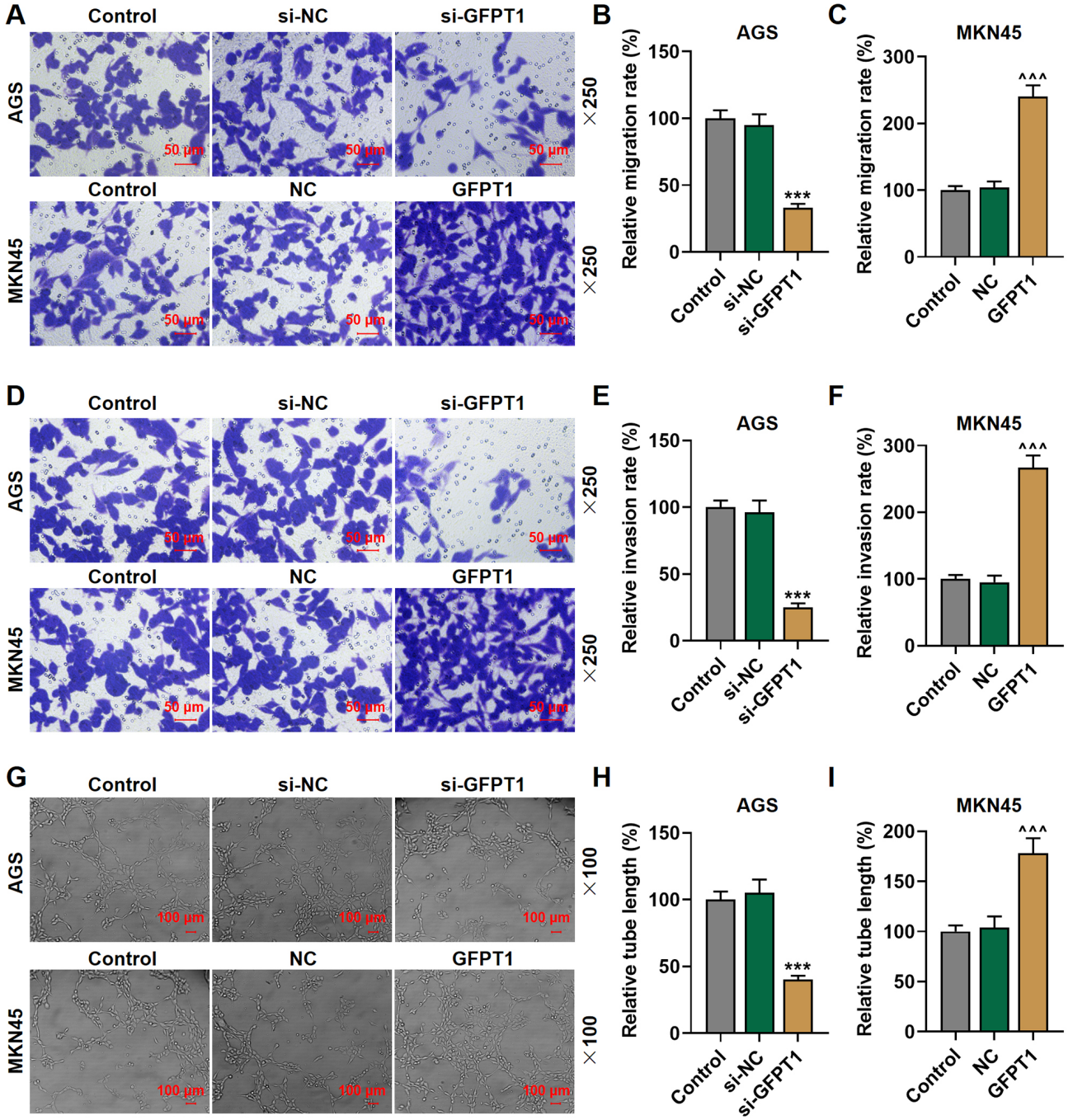

Fig. 3. Effects of *GFPT1* on migration, invasion and angiogenesis of gastric cancer cells. AGS and MKN45 cells received transfection of si-*GFPT1* and *GFPT1* overexpression plasmid, respectively. (A–C) Effects of *GFPT1* on AGS and MKN45 cell migration (transwell migration assay) (magnification: ×250; scale: 50 μm). (D–F) Effects of *GFPT1* on AGS and MKN45 cell invasion (transwell invasion assay) (magnification: ×250; scale: 50 μm). (G–I) Effects of *GFPT1* on AGS and MKN45 cell angiogenesis capacity (angiogenesis assay) (magnification: ×100; scale: 100 μm). $^{\wedge\wedge\wedge}p < 0.001$, $***p < 0.001$; * vs si-NC, $^{\wedge}$ vs NC. n = 3. Abbreviation: *GFPT1*, glutamine-fructose-6-phosphate transaminase 1; NC, negative control.

si-*GFPT1*+NC ($p < 0.01$, Fig. 6G,H). Additionally, the length of blood vessels generated by co-culturing HUVEC with MKN45 cells transfected with NC+si-*KDM4C* was reduced but increased by transfection with *GFPT1*+si-NC ($p < 0.001$, Fig. 6G,I). MKN45 cells in the *GFPT1*+si-*KDM4C* group produced blood vessels that were notably longer than those in the NC+si-*KDM4C* group, and significantly shorter than those in the *GFPT1*+si-NC group ($p < 0.001$, Fig. 6G,I).

Western blot analysis was employed to quantify the levels of Ki67, E-cadherin, N-cadherin, Vimentin, VE-cadherin, and EphA2. In AGS cells, the si-*GFPT1*+NC

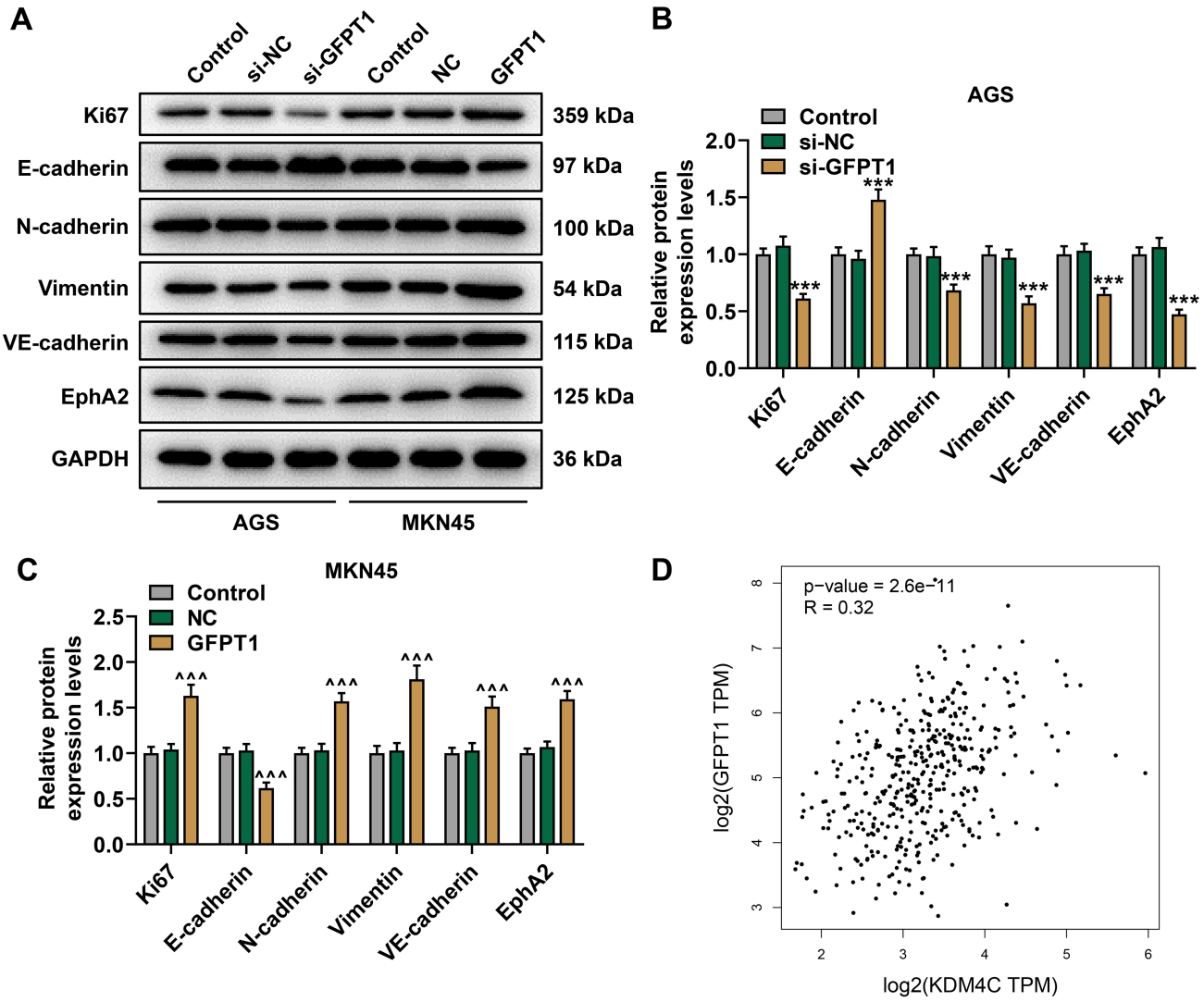

Fig. 4. Effects of *GFPT1* on the expressions of proliferation/EMT-related proteins in AGS and MKN45 cells. AGS and MKN45 cells received transfection of si-*GFPT1* and *GFPT1* overexpression plasmid, respectively. (A–C) Expressions of proliferation- and EMT-related proteins in AGS and MKN45 cells (Western blot). (D) Prediction of the relationship between *KDM4C* and *GFPT1* expressions in gastric cancer (GEPIA database). ^^^$p < 0.001$, ***$p < 0.001$; * vs si-NC, ^ vs NC. n = 3. Abbreviation: *GFPT1*, glutamine-fructose-6-phosphate transaminase 1; NC, negative control; EMT, epithelial-mesenchymal transition.

group exhibited decreased levels of Ki67, N-cadherin, Vimentin, VE-cadherin, and EphA2, while the level of E-cadherin was elevated. Conversely, the si-NC+*KDM4C* group showed opposite trends ($p < 0.01$, Fig. 7A,B). Notably, *KDM4C* overexpression and *GFPT1* deficiency mutually reversed their effects on the expression of these proteins ($p < 0.001$, Fig. 7A,B). In MKN45 cells, the NC+si-*KDM4C* group displayed decreased levels of Ki67, N-cadherin, Vimentin, VE-cadherin, and EphA2 ($p < 0.01$, Fig. 7C,D), and an increased level of E-cadherin ($p < 0.05$, Fig. 7C,D). Conversely, the *GFPT1*+si-NC group showed opposite trends ($p < 0.01$; $p < 0.05$, Fig. 7C,D). Furthermore, *KDM4C* silencing countered the influence of *GFPT1* overexpression on these proteins, and vice versa ($p < 0.05$, Fig. 7C,D).

Discussion

Gastric cancer ranks among frequent tumors affecting the digestive tract, with approximately one million cases reported annually worldwide [21]. Due to delayed detection and absence of early-stage symptoms, less than 20% of patients with advanced gastric cancer survive for five years on average [22]. Numerous studies on the prognosis of cancer patients and innovative adjuvant treatment approaches have been undertaken recently. Molecular targeted therapy, in particular, has emerged as an effective treatment option for gastric cancer [23].

Cancer is characterized by abnormal glucose metabolism [24], and the HBP plays a crucial role in cellular metabolism. *GFPT1*, the first and rate-limiting

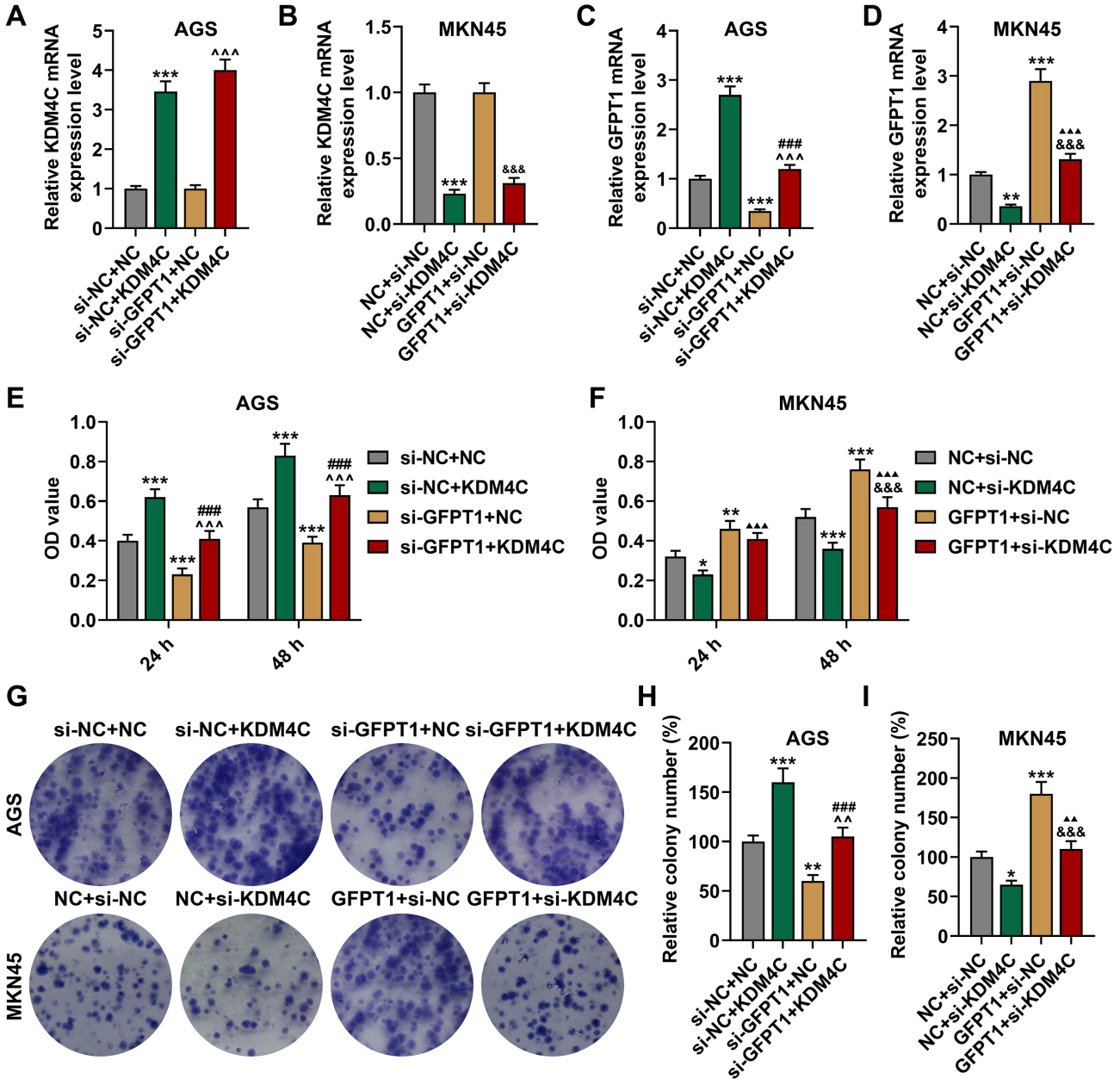

Fig. 5. Effects of *GFPT1* on gastric cancer cell viability and proliferation under the regulation of *KDM4C*. AGS cells experienced transfection of si-NC+NC/si-NC+*KDM4C*/si-*GFPT1*+NC/si-*GFPT1*+*KDM4C*. MKN45 cells experienced transfection of NC+si-NC/NC+si-*KDM4C*/*GFPT1*+si-NC/*GFPT1*+si-*KDM4C*. (A,B) *KDM4C* level in AGS and MKN45 cells (qRT-PCR). (C,D) *GFPT1* level in AGS and MKN45 cells (qRT-PCR). (E,F) Effects of *GFPT1* and *KDM4C* on AGS and MKN45 cell viability (CCK-8 assay). (G–I) Effects of *GFPT1* and *KDM4C* on AGS and MKN45 cell proliferation (colony-forming assay). $^{***}p < 0.001$, $^{**}p < 0.01$, $^{*}p < 0.05$, $^{\wedge\wedge\wedge}p < 0.001$, $^{\wedge\wedge}p < 0.01$, $^{\&\&\&}p < 0.001$, $^{\#\#\#}p < 0.001$, $^{\blacktriangle\blacktriangle\blacktriangle}p < 0.001$, $^{\blacktriangle\blacktriangle}p < 0.01$; *vs si-NC+NC, $^{\wedge}$vs si-*GFPT1*+NC, $^{\#}$ vs si-NC+*KDM4C*, $^{\&}$ vs *GFPT1*+si-NC, $^{\blacktriangle}$ vs NC+si-*KDM4C*. n = 3. Abbreviation: *KDM4C*, Lysine demethylase 4C; *GFPT1*, glutamine-fructose-6-phosphate transaminase 1; NC, negative control; qRT-PCR, quantitative real-time polymerase chain reaction; CCK-8, Cell Counting Kit-8.

enzyme of the HBP, regulates glucose entry and converts it to UDP-GlcNAc [25]. Elevated *GFPT1* expression pattern has been associated with the progression of various cancers, including pancreatic cancer tissues [26], cervical cancer [27], and esophageal cancer [8]. Our study confirmed the upregulation of *GFPT1* in gastric cancer cell lines, where its overexpression promoted cell viability, proliferation, migration, invasion, and vasculogenic mimicry, while *GFPT1* knockdown had the opposite effect. Additionally, we observed that *GFPT1* overexpression increased the expression of proliferation marker Ki67 while *GFPT1* knockdown can decrease the level of proliferation-related protein Ki67.

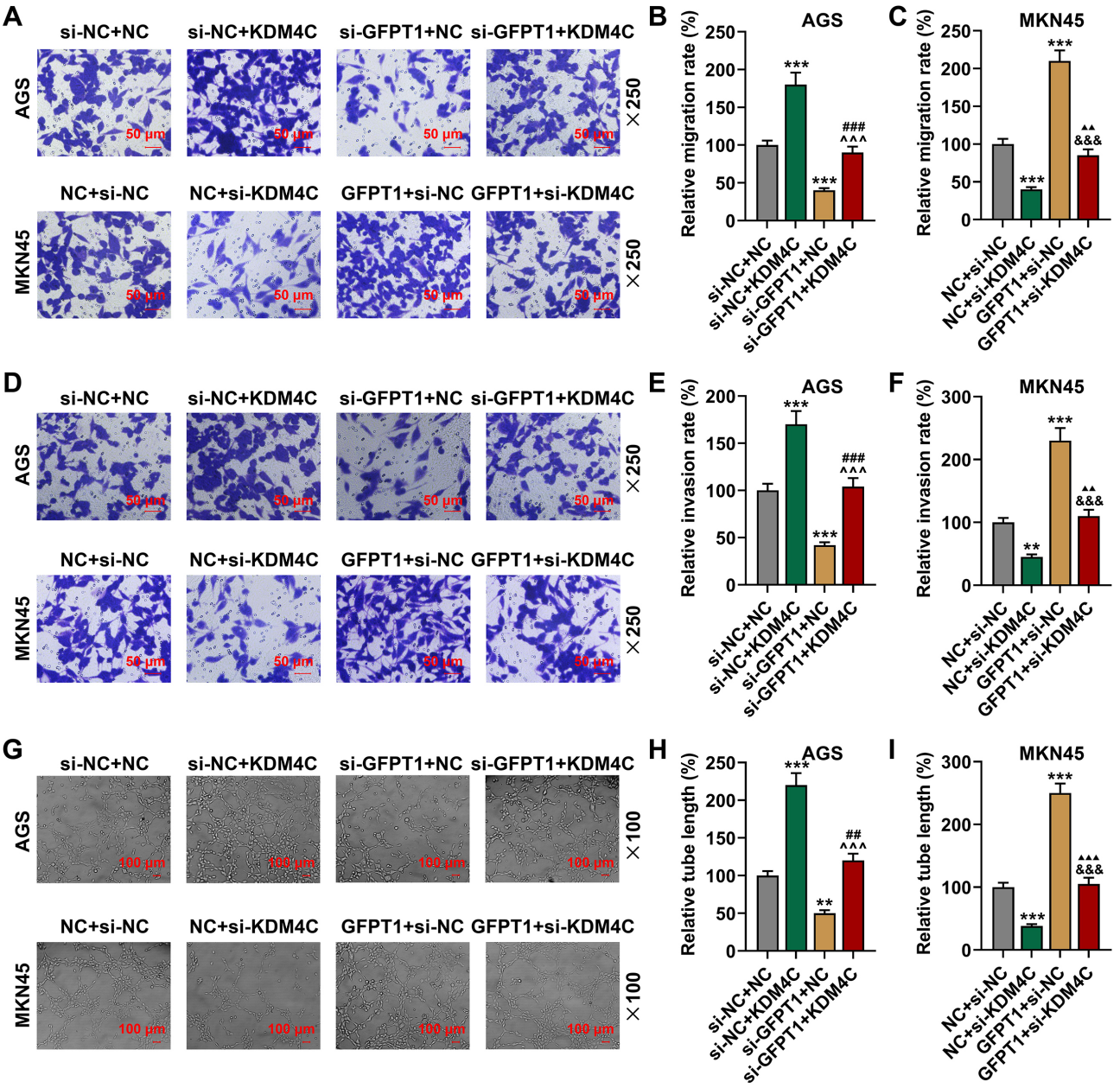

Fig. 6. Effects of *GFPT1* on gastric cancer cell migration, invasion and angiogenesis under the regulation of *KDM4C*. AGS cells experienced transfection of si-NC+NC/si-NC+*KDM4C*/si-*GFPT1*+NC/si-*GFPT1*+*KDM4C*. MKN45 cells experienced transfection of NC+si-NC/NC+si-*KDM4C*/*GFPT1*+si-NC/*GFPT1*+si-*KDM4C*. (A–C) Effects of *GFPT1* on AGS and MKN45 cell migration under the regulation of *KDM4C* (transwell migration assay) (magnification: ×250; scale: 50 μm). (D–F) Effects of *GFPT1* on AGS and MKN45 cell invasion under the regulation of *KDM4C* (transwell invasion assay) (magnification: ×250; scale: 50 μm). (G–I) Effects of *GFPT1* on AGS and MKN45 cell angiogenesis under the regulation of *KDM4C* (angiogenesis assay) (magnification: ×100; scale: 100 μm). $^{***}p < 0.001$, $^{**}p < 0.01$, $^{\wedge\wedge\wedge}p < 0.001$, $^{\#\#\#}p < 0.001$, $^{\#\#}p < 0.01$, $^{\&\&\&}p < 0.001$, $^{\blacktriangle\blacktriangle\blacktriangle}p < 0.001$, $^{\blacktriangle\blacktriangle}p < 0.01$; * vs si-NC+NC, $^{\wedge}$ vs si-*GFPT1*+NC, $^{\#}$ vs si-NC+*KDM4C*, $^{\&}$ vs *GFPT1*+si-NC, $^{\blacktriangle}$ vs NC+si-*KDM4C*. n = 3. Abbreviation: *KDM4C*, Lysine demethylase 4C; *GFPT1*, glutamine-fructose-6-phosphate transaminase 1; NC, negative control.

EMT is a critical process in cancer progression, enhancing cell proliferation, invasion, and metastasis [6]. During EMT, cancer cells undergo molecular changes, such as downregulation of E-cadherin (epithelial marker) and upregulation of N-cadherin and Vimentin (mesenchymal markers) [28], consistent with our findings. We found that overexpression of *GFPT1* can facilitate gastric cancer development by enhancing proliferation and EMT in gastric cancer cells. However, whether *GFPT1* promotes gastric cancer cell proliferation, invasion and vasculogenic mimicry through the EMT requires further investigation.

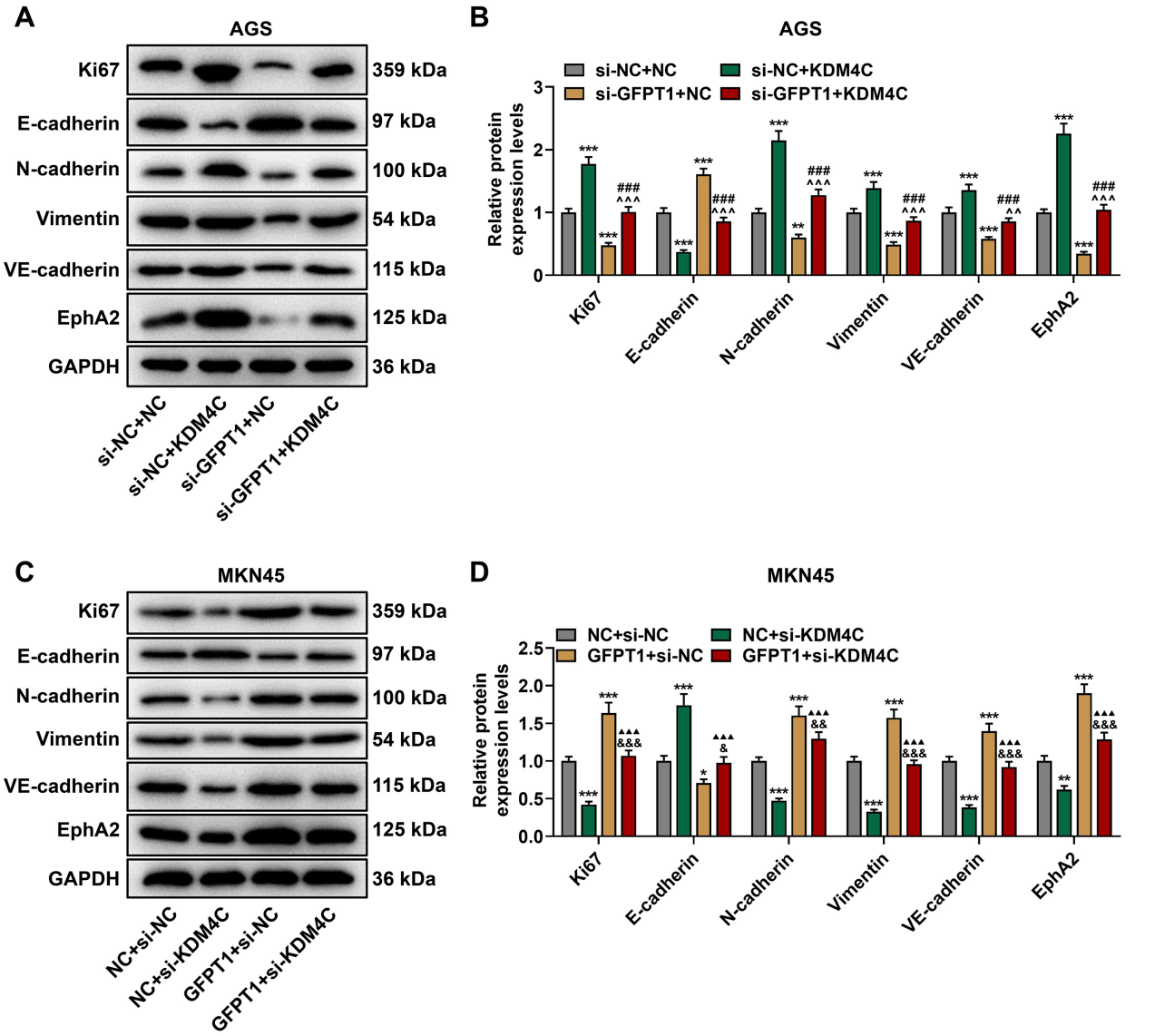

Fig. 7. The effect of *GFPT1* on expressions of proliferation/EMT-related proteins in gastric cancer cells under the regulation of *KDM4C*. AGS cells experienced transfection of si-NC+NC/si-NC+*KDM4C*/si-*GFPT1*+NC/si-*GFPT1*+*KDM4C*. MKN45 cells experienced transfection of NC+si-NC/NC+si-*KDM4C*/*GFPT1*+si-NC/*GFPT1*+si-*KDM4C*. (A–D) Effects of *GFPT1* and *KDM4C* on proliferation/EMT-related proteins in AGS and MKN45 cells under the regulation of *KDM4C* (Western blot). $^{***}p < 0.001$, $^{**}p < 0.01$, $^{*}p < 0.05$, $^{\wedge\wedge\wedge}p < 0.001$, $^{\wedge\wedge}p < 0.01$, $^{\#\#\#}p < 0.001$, $^{\&\&\&}p < 0.001$, $^{\&\&}p < 0.01$, $^{\&}p < 0.05$, $^{\blacktriangle\blacktriangle\blacktriangle}p < 0.001$; * vs si-NC+NC, $^{\wedge}$ vs si-*GFPT1*+NC, $^{\#}$ vs si-NC+*KDM4C*, $^{\&}$ vs *GFPT1*+si-NC, $^{\blacktriangle}$ vs NC+si-*KDM4C*. n = 3. Abbreviation: *KDM4C*, Lysine demethylase 4C; *GFPT1*, glutamine-fructose-6-phosphate transaminase 1; NC, negative control; EMT, epithelial-mesenchymal transition.

Recent advances in epigenetic research have significantly enhanced our comprehension of the etiology and progression of gastric cancer, while also paving the way for the development of novel treatments targeting histone methylation have also been developed [29]. Database predictions have highlighted the enrichment of histone methylation enrichment within the *GFPT1* promoter region. Notably, H3K36me3 was found to exhibit the highest enrichment, with its associated transferase *KDM4C* also being enriched in the *GFPT1* promoter region. Studies have shown that H3K36me3 plays a crucial role in maintaining an active chromatin state, facilitating transcription elongation, and enhancing gene transcription levels [30,31]. Furthermore, *KDM4C*, known for its involvement in demethylating histones, has been implicated in initiating metabolic reprogramming, controlling B cell activation, and promoting cell growth [32].

The gastric cancer tissues have a high expression of *KDM4C*, which helps with the maintenance of cancer cell stemness [19]. Therefore, the influence of *KDM4C*-regulated *GFPT1* on gastric cancer was detected. The findings revealed that *KDM4C* exerted a detrimental effect on

the viability, proliferation, migration, invasion, and vasculogenic mimicry of gastric cancer cells. Concurrently, *KDM4C* was observed to downregulate E-cadherin expression while upregulating Ki67, N-cadherin, Vimentin, VE-cadherin, and EphA2 expressions, indicating its role in promoting gastric cancer cell proliferation and EMT. This study elucidates the contribution of *KDM4C* to *GFPT1* expression and the onset of gastric cancer. Interestingly, while *GFPT1* did not regulate *KDM4C* expression directly, it modulated the functional impact of *KDM4C* on gastric cancer cell phenotypes. This suggests a potential upstream regulatory role of *KDM4C* on *GFPT1* in gastric cancer.

Noteworthily, there are some limitations in this study. It is still uncertain whether *KDM4C* directly regulates *GFPT1* in gastric cancer cells or indirectly regulates it by affecting another signaling pathway. Besides, there is a lack of *in vivo* validation. Therefore, more experimental designs and time-course experiments are required to fully expound our findings.

In summary, *KDM4C* positively regulated *GFPT1* to improve the viability, proliferation, migration, invasion, and vasculogenic mimicry of gastric cancer cells, and promote EMT to aggravate gastric cancer.

Conclusion

Gastric cancer exhibits a complex pathogenesis. In recent years, researchers have explored its etiology from various angles, prioritizing the identification of pathways for potential solutions. This study focuses on the cancer-related gene *GFPT1* and unveils its role in promoting gastric cancer growth, along with the positive regulatory influence of *KDM4C* on *GFPT1*. Suppressing either *GFPT1* or *KDM4C* shows promise in impeding gastric cancer development, thus providing a novel therapeutic avenue for future exploration.

Availability of Data and Materials

The analyzed data sets generated during the study are available from the corresponding author upon reasonable request.

Author Contributions

CKL and YQC designed the research study; HJD, QYX, and WYZ performed the research; HJD, QYX, and WYZ collected and analyzed the data. All authors have been involved in drafting the manuscript and all authors have been involved in revising it critically for important intellectual content. All authors have given final approval of the version to be published. All authors have participated sufficiently in the work to take public responsibility for appropriate portions of the content and agreed to be accountable for all aspects of the work in ensuring that questions related to its accuracy or integrity.

Ethics Approval and Consent to Participate

Not applicable.

Acknowledgment

Not applicable.

Funding

This research received no external funding.

Conflict of Interest

The authors declare no conflict of interest.

References

[1] Bray F, Ferlay J, Soerjomataram I, Siegel RL, Torre LA, Jemal A. Global cancer statistics 2018: GLOBOCAN estimates of incidence and mortality worldwide for 36 cancers in 185 countries. CA: a Cancer Journal for Clinicians. 2018; 68: 394–424.

[2] Koulis A, Buckle A, Boussioutas A. Premalignant lesions and gastric cancer: Current understanding. World Journal of Gastrointestinal Oncology. 2019; 11: 665–678.

[3] Sexton RE, Al Hallak MN, Diab M, Azmi AS. Gastric cancer: a comprehensive review of current and future treatment strategies. Cancer Metastasis Reviews. 2020; 39: 1179–1203.

[4] Yang K, Lu L, Liu H, Wang X, Gao Y, Yang L, *et al*. A comprehensive update on early gastric cancer: defining terms, etiology, and alarming risk factors. Expert Review of Gastroenterology & Hepatology. 2021; 15: 255–273.

[5] Wong SHM, Fang CM, Chuah LH, Leong CO, Ngai SC. E-cadherin: Its dysregulation in carcinogenesis and clinical implications. Critical Reviews in Oncology/hematology. 2018; 121: 11–22.

[6] Dongre A, Weinberg RA. New insights into the mechanisms of epithelial-mesenchymal transition and implications for cancer. Nature Reviews. Molecular Cell Biology. 2019; 20: 69–84.

[7] Lam C, Low JY, Tran PT, Wang H. The hexosamine biosynthetic pathway and cancer: Current knowledge and future therapeutic strategies. Cancer Letters. 2021; 503: 11–18.

[8] Zhang C, Lian H, Xie L, Yin N, Cui Y. LncRNA ELFN1-AS1 promotes esophageal cancer progression by up-regulating GFPT1 via sponging miR-183-3p. Biological Chemistry. 2020; 401: 1053–1061.

[9] Zhang Y, Li J, Huang Y, Chen Y, Luo Z, Huang H, *et al*. Improved antitumor activity against prostate cancer via synergistic targeting of Myc and GFAT-1. Theranostics. 2023; 13: 578–595.

[10] Huang H, Wang Y, Huang T, Wang L, Liu Y, Wu Q, *et al*. FOXA2 inhibits doxorubicin-induced apoptosis via transcriptionally activating HBP rate-limiting enzyme GFPT1 in HCC cells. Journal of Physiology and Biochemistry. 2021; 77: 625–638.

[11] Wang Y, Zhao X, Li J, Wang X, Hu W, Zhang X. Four m6A RNA Methylation Gene Signatures and Their Prognostic Values in Lung Adenocarcinoma. Technology in Cancer Research & Treatment. 2022; 21: 15330338221085373.

[12] Xiao C, Fan T, Tian H, Zheng Y, Zhou Z, Li S, *et al*. H3K36 trimethylation-mediated biological functions in cancer. Clinical Epigenetics. 2021; 13: 199.

[13] Zhang Y, Sun Z, Jia J, Du T, Zhang N, Tang Y, *et al*. Overview of Histone Modification. Advances in Experimental Medicine and Biology. 2021; 1283: 1–16.

[14] Xu Q, Xiang Y, Wang Q, Wang L, Brind'Amour J, Bogutz AB, *et al*. SETD2 regulates the maternal epigenome, genomic imprinting and embryonic development. Nature Genetics. 2019; 51: 844–856.
[15] Hu M, Hu M, Zhang Q, Lai J, Liu X. SETD2, an epigenetic tumor suppressor: a focused review on GI tumor. Frontiers in Bioscience (Landmark Edition). 2020; 25: 781–797.
[16] Chen R, Zhao WQ, Fang C, Yang X, Ji M. Histone methyltransferase SETD2: a potential tumor suppressor in solid cancers. Journal of Cancer. 2020; 11: 3349–3356.
[17] González-Rodríguez P, Engskog-Vlachos P, Zhang H, Murgoci AN, Zerdes I, Joseph B. SETD2 mutation in renal clear cell carcinoma suppresses autophagy via regulation of ATG12. Cell Death & Disease. 2020; 11: 69.
[18] Lin CY, Wang BJ, Chen BC, Tseng JC, Jiang SS, Tsai KK, *et al*. Histone Demethylase KDM4C Stimulates the Proliferation of Prostate Cancer Cells via Activation of AKT and c-Myc. Cancers. 2019; 11: 1785.
[19] Lang T, Xu J, Zhou L, Zhang Z, Ma X, Gu J, *et al*. Disruption of KDM4C-ALDH1A3 feed-forward loop inhibits stemness, tumorigenesis and chemoresistance of gastric cancer stem cells. Signal Transduction and Targeted Therapy. 2021; 6: 336.
[20] Almeida KC, Pereira AF, Alcântara Neto AS, Avelar SRG, Bertolini LR, Bertolini M, *et al*. Real-time qRT-PCR analysis of EGF receptor in cumulus-oocyte complexes recovered by laparoscopy in hormonally treated goats. Zygote (Cambridge, England). 2011; 19: 127–136.
[21] Strong VE. Progress in gastric cancer. Updates in Surgery. 2018; 70: 157–159.
[22] Huo J, Wu L, Zang Y. Eleven immune-gene pairs signature associated with TP53 predicting the overall survival of gastric cancer: a retrospective analysis of large sample and multicenter from public database. Journal of Translational Medicine. 2021; 19: 183.
[23] Lin S, Liu J, Jiang W, Wang P, Sun C, Wang X, *et al*. METTL3 Promotes the Proliferation and Mobility of Gastric Cancer Cells. Open Medicine (Warsaw, Poland). 2019; 14: 25–31.
[24] Hanahan D, Weinberg RA. Hallmarks of cancer: the next generation. Cell. 2011; 144: 646–674.
[25] Akella NM, Ciraku L, Reginato MJ. Fueling the fire: emerging role of the hexosamine biosynthetic pathway in cancer. BMC Biology. 2019; 17: 52.
[26] Gong Y, Qian Y, Luo G, Liu Y, Wang R, Deng S, *et al*. High GFPT1 expression predicts unfavorable outcomes in patients with resectable pancreatic ductal adenocarcinoma. World Journal of Surgical Oncology. 2021; 19: 35.
[27] Li D, Guan M, Cao X, Zha ZQ, Zhang P, Xiang H, *et al*. GFPT1 promotes the proliferation of cervical cancer via regulating the ubiquitination and degradation of PTEN. Carcinogenesis. 2022; 43: 969–979.
[28] Mittal V. Epithelial Mesenchymal Transition in Tumor Metastasis. Annual Review of Pathology. 2018; 13: 395–412.
[29] Sokolova O, Naumann M. Crosstalk Between DNA Damage and Inflammation in the Multiple Steps of Gastric Carcinogenesis. Current Topics in Microbiology and Immunology. 2019; 421: 107–137.
[30] He J, Xu T, Zhao F, Guo J, Hu Q. SETD2-H3K36ME3: an important bridge between the environment and tumors. Frontiers in Genetics. 2023; 14: 1204463.
[31] Sen P, Dang W, Donahue G, Dai J, Dorsey J, Cao X, *et al*. H3K36 methylation promotes longevity by enhancing transcriptional fidelity. Genes & Development. 2015; 29: 1362–1376.
[32] Jie X, Fong WP, Zhou R, Zhao Y, Zhao Y, Meng R, *et al*. USP9X-mediated KDM4C deubiquitination promotes lung cancer radioresistance by epigenetically inducing TGF-β2 transcription. Cell Death and Differentiation. 2021; 28: 2095–2111.